

# AMT Measurements for MODIS Calibration and Validation

Stanford B. Hooker  
*NASA Goddard Space Flight Center*  
*SeaWiFS Project Code 970.2*  
*Greenbelt, Maryland*

## Background and Introduction

Ocean color satellite missions, like the Sea-viewing Wide Field-of-view Sensor (SeaWiFS) or the Moderate Resolution Imaging Spectroradiometer (MODIS) projects, are tasked with acquiring a global ocean color data set, validating and monitoring the accuracy and quality of the data, processing the radiometric data into geophysical units using a set of atmospheric and bio-optical algorithms, and distributing the final products to the scientific community. The long-standing objective of the SeaWiFS Project, for example, is to produce water-leaving radiances to within 5% absolute (Hooker and Esaias 1993).

The accurate determination of upper ocean apparent optical properties (AOPs) is essential for the vicarious calibration of ocean color data and the validation of the derived data products, because the sea-truth measurements are the reference data to which the satellite observations are compared (Hooker and McClain 2000). The uncertainties associated with *in situ* AOP measurements have various sources, such as, the deployment and measurement protocols used in the field, the absolute calibration of the radiometers, the environmental conditions encountered during data collection, the conversion of the light signals to geophysical units in a data processing scheme, and the stability of the radiometers in the harsh environment they are subjected to during transport and use.

In recent years, progress has been made in estimating the magnitude of some of these uncertainties and in defining procedures for minimizing them. For the SeaWiFS Project, the first step was to convene a workshop to draft the SeaWiFS Ocean Optics Protocols. The protocols adhere to the Joint Global Ocean Flux Study (JGOFS) sampling procedures (Joint Global Ocean Flux Study 1991) and define the standards for optical measurements to be used in SeaWiFS radiometric validation and algorithm development (Mueller and Austin 1992). The protocols are periodically updated as deficiencies are identified and outstanding issues are resolved (Mueller and Austin 1995, and Mueller 2000).

The follow-on inquiries into controlling uncertainties investigated a variety of topics. The SeaWiFS Intercalibration Round-Robin Experiment (SIRREX) activity demonstrated that the uncertainties in the traceability between the spectral irradiance of calibration lamps were approximately 1.0%, and the intercomparisons of sphere radiance was approximately 1.5% in absolute spectral radiance and 0.3% in stability (Mueller et al. 1996). The first SeaWiFS Data Analysis Round Robin (DARR-94) showed differences in commonly used data processing methods were about 3–4% of the aggregate mean estimate (Siegel et al. 1995). Hooker and Aiken (1998) made estimates of radiometer stability using the SeaWiFS Quality Monitor (SQM), a portable and stable light source, and showed the stability of radiometers in the field during a 36-day deployment was on average to within 1.0% (although some channels occasionally performed much worse). More recently,

Hooker and Maritorena (2000) quantified differences in the in-water methods and techniques employed for making radiometric measurements and demonstrated a total uncertainty in the measurement of in-water AOPs at approximately the 3% level.

## Open Ocean Results

The SeaWiFS Field Team has combined the collection of ground-truth observations with specific experiments to investigate the sources of uncertainties in AOP measurements. Many of the experiments and data collection opportunities took place during several Atlantic Meridional Transect (AMT) cruises on board the Royal Research Ship *James Clark Ross* (JCR) between England and the Falkland Islands (Aiken et al. 2000). The majority of the AMT data set was from Case-1 conditions and took place from September 1995 to June 1999.

Water-leaving radiances can be derived by extrapolating in-water measurements taken close to the sea surface or obtained directly from above-water measurements. More recently as a part of this activity, additional experiments and data collection activities have been executed to extend the AMT predominantly in-water data set to other open ocean areas and above-water methods. These include a) the *Productivité des Systèmes Océaniques Pélagiques* (PROSOPE) cruise, which took place between 4 September and 4 October 1999; b) a cruise into the Mid-Atlantic Bight, which took place between 24 April and 3 May 2000, and c) two cruises into Exuma Sound, which took place between 24 February and 1 March 2000 as well as 22 February and 1 March 2001.

Although it has not been as extensively validated as the in-water approach, above-water methods for vicarious calibration remain nevertheless attractive, because a) the data can presumably be collected more rapidly and from a ship underway, and b) the frequently turbid and strongly absorbing waters in shallow Case-2 environments impose severe limitations on in-water measurements, particularly because of the instrument self-shading effect.

Above- and in-water measurements of  $L_W(\lambda)$  can be related to one another using the pointing geometry of the sensors, the sun geometry, the (surface) interface transmission, and the so-called  $Q$ -factor. The  $Q$ -factor relates the upward radiance field below the surface with that exiting the surface, the angular bidirectional dependency of these fields, and the transformation of radiance or irradiance into reflectance (Morel and Gentili 1996). In-water measurements of the  $Q$ -factor with nadir-pointing instruments (the usual case) are denoted  $Q_n(\lambda)$  and are calculated as the ratio of the upward irradiance to the upwelling radiance,  $Q_n(\lambda) = E_u(\lambda)/L_u(\lambda)$ .

The data from the most recent cruises agreed well with the AMT data set in terms of the accuracy of the in-water AOP measurements and the uncertainties in inverting the

optical data into chlorophyll *a* concentration using a standard ocean color algorithm, but they also confirmed two inconsistencies in the AMT data set. The first inconsistency was the amplitude and spectral dependence of  $Q_n(\lambda)$  did not agree with theoretical studies. To more completely investigate this result, special so-called *Q*-factor experiments were conducted during the PROSOPE and Mid-Atlantic Bight cruises. In these experiments, sequential casts were made during clear-sky conditions in homogeneous, Case-1 waters during an extensive part of the afternoon (i.e., during a lengthy change in the solar zenith angle,  $\theta$ ). Figure 1 shows the distribution of  $Q_n(\lambda)$  as a function of  $\theta$ . Although the general shape of increasing  $Q_n(\lambda)$  with increasing solar zenith angle is in agreement with theory, the amplitudes are incorrect, and more important, the wavelength dependence is inverted:  $Q_n(\lambda)$  decreases with increasing  $\lambda$ , whereas theory predicts it should decrease.

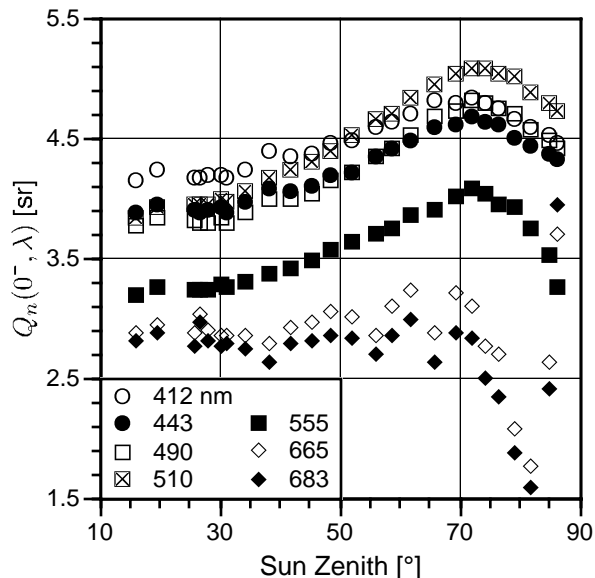


**Fig. 1.** The distribution of  $Q_n(\lambda)$  as a function of the solar zenith angle.

The second inconsistency was the above-water  $L_W(\lambda)$  values collected from a large research vessel disagreed with the in-water values, which were collected simultaneously, by as much as 13–27%. All the field instruments were intercalibrated, and the in-water instruments were floated far away from the ship before any data were recorded, so the most likely explanation for the disagreement was platform contamination in the above-water data.

This possibility was analyzed by devising a diagnostic parameter,  $r(865)$ , based on the principles involved in the formulation of two above-water methods: Morel (1980) and the SeaWiFS Ocean Optics Protocols (Mueller and Austin 1995), hereafter referred to as M80 and S95, respectively. When using an above-water method, the total radiance measured above the sea surface,  $L_T(\lambda)$ , includes the wanted information,  $L_W(\lambda)$ , plus a contamination term,

$\Delta L$ , originating from light reflected by the sea surface and into the sensor:

$$L_T(\lambda) = L_W(\lambda) + \Delta L, \quad (1)$$

where the pointing requirements have been omitted.

The processing of above-water data consists of removing the contamination term,  $\Delta L$  in (1), which adds to the marine signal and originates from reflections at the air–sea interface. The sky radiance,  $L_i(\lambda)$ , reflected off the wave-roughened surface into the detector is *a priori* at the origin of the  $\Delta L$  signal. Reflected radiation from the sampling platform is, however, another source of contamination. Even if only the sky reflection is considered, its contribution to  $L_T(\lambda)$  is always important.

For Case-1 waters, in the near-infrared domain (e.g., at 780 and 865 nm) where the sea is essentially *black*, this contribution amounts to 100%, and decreases toward short wavelengths where the diffuse ocean reflectance departs from zero. In Case-2 waters, particularly when the sediment load is high, the water reflectance may deviate from zero in the near infrared and contribute to the  $\Delta L$  signal.

The M80 glint correction method is based on the existence of a black target in the near-infrared region at a reference wavelength,  $\lambda_r$ . The above-water radiance measured at  $\lambda_r$  is entirely due to surface reflection, and this estimate is extended over the whole spectrum by using the spectral dependence of the incident sky radiance measured in the direction appropriate for reflection from the sea surface. Estimated glint is subtracted from the total signal to recover  $L_W(\lambda)$ . The S95 method makes use of the same set of measurements, but they are used differently. The glint is removed through a constant interface reflectance factor,  $\rho$ , which is applied to all the spectral sky radiances; in general,  $\rho$  depends on the capillary wave slopes, and, thus, on wind speed (Austin 1974 and Mobley 1999).

A comparison of the output of the M80 and S95 correction methods allows the detection of any ship contamination in the  $L_T(\lambda)$  signal in Case-1 waters. This is because the M80 method is sensitive to, and, thus, is able to identify a ship perturbation, whereas the S95 method, based on a theoretical value of the reflectance factor, will just ignore it. The presence of a ship perturbation can be detected with the ratio

$$r(865) = \frac{L_T(865)/L_i(865)}{\rho} \quad (2)$$

where the numerator comes from M80 and the denominator from S95. Under normal circumstances, i.e., in the absence of a ship perturbation,  $r(865) = 1$ , within the accepted variance (and provided that  $\rho$  is given a correct value). Any other reflected radiation added to the sky-reflected radiation will lead to  $r(865) > 1$ , and the departure from unity is an estimate of this effect. Figure 2 presents the  $r(865)$  values for the PROSOPE cruise plotted as a function of the pointing angle of the above-water radiometers with respect to the side of the ship,  $\alpha$ .

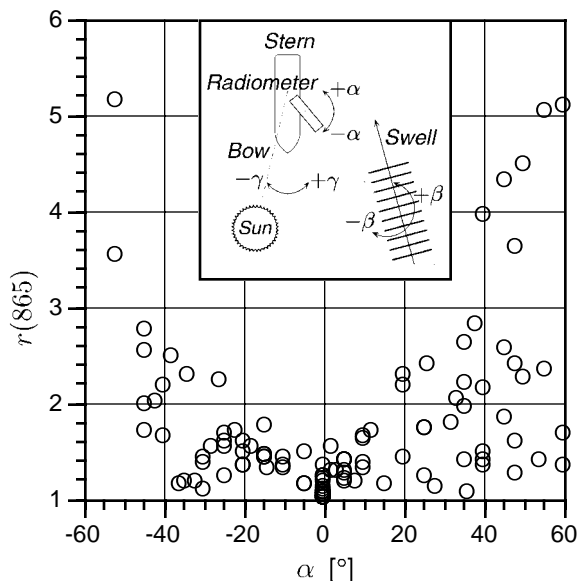


**Fig. 2.** The distribution of  $r(865)$  as a function of  $\alpha$  (negative  $\alpha$  values are towards the bow and positive  $\alpha$  values towards the stern). Out of the total data set of 128 casts, 19 were in overcast conditions and 109 were in clear-sky conditions; overcast data are not shown as separate symbols, because they fall within a narrow range (slightly larger than 1) and all at  $\alpha = 0$ , so they would obscure the clear-sky results. The inset panel shows the pointing angle of the above-water radiometers with respect to the ambient swell ( $\beta$ ), and the angle of the sun with respect to the bow ( $\gamma$ ).

Although the PROPOSED data set was composed of 137 simultaneous above- and in-water casts, 9 were excluded because of unanticipated cloud interference, ship movement during the cast, etc. The remaining 128 casts provide a good distribution of data with respect to  $\alpha$ , and show that when the instrument is pointed perpendicular to the side of the ship ( $\alpha = 0$ ), the  $r(865)$  values are a little larger than 1, which suggests a reduced contamination by the ship. As the radiometers are pointed more and more towards the bow or stern, that is when the distance from the ship to the surface spot decreases,  $r(865)$  dramatically increases, reaching values as high as 4–5 when  $\alpha \approx \pm 60^\circ$ . These large ratios indicate the radiation reflected by the surface and seen by the sensor is largely dominated by that originating from the superstructure.

These high values, however, are not observed in a systematic manner. For example, when  $\alpha = 40^\circ$  or  $60^\circ$ ,  $r(865)$  values span the interval 1–5, which deserves another kind of analysis, involving  $\gamma$ , i.e., the angle between the center line of the ship and the position of the sun (Fig. 2 inset panel). According to the sign of  $\gamma$ , the port side of the ship (where the above-water radiometers were installed) is, or is not, illuminated by the sun, which makes a difference in the intensity (and spectral composition) of the light reflected from the superstructure.

An analysis of  $r(865)$  as a function of  $\gamma$  shows the contamination effects of the ship are reduced when the side from which the sensor is operated is in shadow, so that the superstructure is only illuminated by the sky radiation (or by uniform clouds); the contamination increases when the port side is sunlit, or if the bridge is sunlit (when  $\gamma$  is small). The geometrical aspect of the contamination is not surprising; more surprising is the importance of the effect and its complexity related to the shape of the superstructure. As with many ships, elements of the forward superstructure on the research vessel used during PROSOPE sloped to the sides of the vessel which provided reflection opportunities under a variety of sun geometries with respect to the bow.

Although not as significant as the sun geometry, the effects of surface gravity waves on the above-water measurements were quantifiable: a) measurements along the wave troughs are a significant local minimum, which means they are radiometrically darker than the wave crests at all wavelengths; b) the darkening effect is the largest at 412 and 555 nm; and c) at 510–555 nm, a converse trend (i.e., a brightening) seems to occur.

## Coastal Ocean Results

The PROSOPE above-water data were collected with instruments fixed to the pointing assembly. Although the instruments could be pointed to arbitrary angles in the vertical and horizontal planes, they were sufficiently large that they could not be safely operated at very high points on a ship's superstructure, particularly in high sea states. In anticipation of working on smaller boats in coastal waters, a very small system that could be gimballed and, thus, would not be as negatively influenced by ship motion was developed. This required the SeaWiFS Field Team to fund the development of a new class of optical sensors that are significantly smaller and lighter than those currently available. These new sensors are manufactured by Satlantic, Inc. (Halifax, Canada) and are referred to as the OCR-500 series of instruments.

The new above-water instrument is called the micro Surface Acquisition System (microSAS) and is pictured in Fig. 3. The above-water radiometers are mounted on movable plates contained within a gimbal. The plates can be set to an arbitrary vertical (nadir or zenith) angle with respect to the horizontal plane between  $0$ – $50^\circ$  (most data is currently collected at  $40^\circ$ ). In addition, the entire sensor assembly can be rotated to arbitrary azimuthal viewing angles to within  $0.5^\circ$ . A sun compass at the top of the assembly allows for easy pointing of the instrument to  $\pm 90^\circ$  (in  $15^\circ$  increments) with respect to the solar plane. The ballast for the gimbal contains a compass with built in tilt and roll sensors. The latter ensure confirmation of the vertical orientation of the sensors during data acquisition and permit fine tuning (ballasting and tensioning) of the gimbal structure in any sea state.



**Fig. 3.** The microSAS instrument composed of the upward-pointing  $L_i$  sensor and the downward-pointing  $L_T$  sensor. The ballast, containing the compass with tilt and roll sensors, is the large black cylinder below the gimbal plane.

The Italian Coastal Atmosphere and Sea Time-Series (CoASTS) project is a cooperative activity between the European Joint Research Centre (JRC) and the Italian National Research Council (CNR). As part of the field campaigns, which started in October 1995 and continue to-date, atmospheric and marine measurements are periodically performed at the *Acqua Alta* Oceanographic Tower (AAOT). The tower is located in the northern Adriatic Sea approximately 15 km southeast of the city of Venice in approximately 17 m of water (Zibordi et al. 1999).

The SeaWiFS Photometer Revision for Incident Surface Measurements (SeaPRISM) was conceived by the SeaWiFS Field Team, and developed by the JRC and CIMEL Electronique (Paris, France). SeaPRISM is based on a CE-318 sun photometer which is an automatic system that measures the direct sun irradiance plus the sky radiance in the sun and almucantar planes (Hooker et al. 2000). The revision to the CE-318 that makes the instrument useful for ocean color activities is a capability for measuring the sea surface using the M80 and S95 methods. What makes this instrument particularly powerful is it can operate autonomously, so a sampling site can be continuously monitored in between field campaigns that completely characterize the bio-optical conditions of the site.

A prototype SeaPRISM was successfully deployed for a one-year period at the AAOT which was compared to simultaneous deployments of an in-water system (Zibordi

et al. 2001). The SeaPRISM measurements showed a slope in the least-squares linear regression fit equal to 1.05 with a determination coefficient of 0.99. More specifically, the intercomparisons exhibited average unbiased percentage difference (UPD†) values of 6.9, 7.2, and 23.0% at 440, 500, and 670 nm, respectively; the intercomparison of the water-leaving radiance ratios,  $L_W(440)/L_W(500)$ , exhibited a UPD of 5.3%.

The success of the prototype SeaPRISM system has led to a plan to deploy a small number of production SeaPRISM units at a variety of offshore oil and gas platforms in the Adriatic Sea south of the AAOT. The towers are in different water depths and typical water regimes than the AAOT, so the small network will provide an unprecedented description of the coastal ocean and atmosphere with autonomous instruments. The above-water results achieved with the open ocean analyses (Fig. 2), however, suggest an analysis of platform perturbations on the above-water measurements is needed.

In preparation for a tower perturbation experiment, the JRC developed an extensible deployment system for a lightweight above-water system (Fig. 4). The extensible system was composed of a tubular box frame that was connected together with prefabricated sections. The box frame was approximately 25 m long and could be extended away from the tower approximately 11 m (at a 10 m extension, the frame sagged approximately  $1^\circ$ ). The microSAS instrument was mounted to the end of the frame, and was positioned with respect to the sun before the frame was extended the desired distance away from the tower. The gimbal ensured the sensors achieved a horizontal reference (to within  $\pm 0.5^\circ$ ) after the frame was positioned. The frame was moved in and out by hand, guided by rollers mounted within a series of square supports.

The basic experimental plan was to make a series of above-water measurements in 1 m increments with respect to the tower (usually 10 incremental measurements were made), all the while observing the pointing requirements with respect to the sun ( $90^\circ$  with respect to the sun). The latter ensured that a variety of viewing distances with respect to the tower base were collected. The experiment took place from 18–29 June 2001 during predominantly clear skies. A total of 42 experiments were conducted composed of 435 individual above-water casts (3 min measurement sequences).

The space series of sequential measurements will be compared to the farthest viewing point to see if there is an increasing perturbation in the above-water data as the measurements are made closer and closer to the tower base. The above-water data will also be compared to a variety of in-water measurements (including discrete water filtration samples, inherent optical properties, AOPs, etc.) taken at

† The UPD between  $N$  realizations of two data products  $\mathfrak{F}^A$  and  $\mathfrak{F}^B$  is computed as  $\frac{200}{N} \sum_{i=1}^N \frac{|\mathfrak{F}^A(\lambda) - \mathfrak{F}^B(\lambda)|}{\mathfrak{F}^A(\lambda) + \mathfrak{F}^B(\lambda)}$ .



**Fig. 4.** The extensible deployment system used at the AAOT showing **a)** the box frame fully extended with the microSAS instruments mounted at the end, and **b)** the support system. The box frame is made up of tubular sections commonly used in the construction of aerial towers. The small cross section of the frame, and the fact that it was painted black, ensured a minimum perturbation by the frame on the surface of the water.

the same time; these data will also be used to determine the homogeneity of the water during each experiment.

## Laboratory Measurements

If a total 5% uncertainty level is to be maintained for a vicarious calibration exercise (remote plus *in situ* instrumentation), approximately half of the uncertainty budget, i.e., 2.5% (actually if quadrature sums are used, the ground-truth component is closer to 3.5%), is available for the ground truth component. This means individual contributions of uncertainty must be at approximately the 1% level, which is a state-of-the-art objective. In the investigation of laboratory sources of uncertainty, two uncertainty thresholds were considered: 2.5% as a hoped for minimum (because it represents almost all of the ground truth uncertainty budget), and 1.0% as a needed goal (because it permits some expansion in the other components of the total uncertainty budget).

The poor agreement between *in situ* and theoretical values of  $Q_n(\lambda)$  (Fig. 2) suggests there could be a problem with the in-water data. The accuracy of any AOP determination is a function of the quality of the observational measurement, the data acquisition methodology, and the data processing method employed. The former includes the accuracy of the optical calibration and the radiometric stability of the instruments while they are being used in the field. The data acquisition programs have been rigorously reviewed and tested (including comparisons with commercial software) and show no evidence of data corruption. The stability of the radiometers has been repeatedly

measured and intercompared in the field—with the exception of early instruments constructed with so-called *soft filters* (Hooker and Aiken 1998), they are stable to within 1% and intercompare during simultaneous casts to within 2% (Hooker and Morel 2001). This leaves only optical calibration and data processing as potential problems.

To investigate the possible importance of data processing methods on the final data products, a round-robin intercomparison was organized (Hooker et al. 2001a). Three processors from three different groups were intercompared: the JRC (J), Satlantic (S), and the SeaWiFS Project or GSFC (G). The focus of the round-robin study was the estimation of a variety of commonly used data products derived from two different classes of in-water optical instruments. Eleven parameters important to bio-optical analyses were intercompared. The parameters were calculated for a data set covering a large range of total chlorophyll *a* concentration (0.08–2.43 mg m<sup>-3</sup>). All three processors were intercompared using 40 optical profiles; the JRC and GSFC processors were further intercompared using an additional 10 casts (the larger data set increased the amount of data in very clear waters, thereby extending the lowest total chlorophyll *a* concentration to 0.027 mg m<sup>-3</sup>).

The data were also separated according to the oceanic environment, deep ocean (DO) or shallow coastal (SC), and according to the instrument type, free-fall (FF) profiler or winch and crane (WC) system. The instruments used with these data included the SeaWiFS Optical Profiling System (SeaOPS) and the Low-Cost NASA Environmental Sampling System (LoCNESS) for the former, and the Wire-Stabilized Profiling Environmental Radiometer

(WiSPER) and a variant of the miniature NASA Environmental Sampling System (miniNESS) for the latter. SeaOPS and WiSPER are deployed using a winch and crane, whereas, LoCNESS and miniNESS are floated away from the sampling platform and deployed by hand. The deep ocean data were all from Case-1 conditions, and the shallow coastal data were from Case-2 conditions or from water near the threshold between Case-1 and Case-2 in terms of the Loisel and Morel (1998) classification scheme.

In this study, no one data processing system was assumed to be more correct than another, so the UPD was used for intercomparisons. In terms of overall spectral averages, many of the JRC and GSFC (JG) results intercompared to within 2.5%, but none of the Satlantic results intercompared with the other processors (JS and GS) at this level. Band-ratio averages, however, frequently intercompared to within 2.5% for all processor combinations, even when the overall spectral averages did not. If the JRC and GSFC processor options were made more similar (same extrapolation intervals, data filtering, etc.), the two processors usually intercompared to within 1%. An example of this for the upwelled radiance at null depth,  $L_u(0^-)$ , and the diffuse attenuation coefficient,  $K_d$ , is shown in Fig. 5. These variables were selected, because they are very important to the calibration and validation process:  $L_u(0^-)$  is used directly in calculating  $L_W(\lambda)$ , and  $K_d$  (Fig. 5b) is the most common variable to describe the attenuation of light in the upper layers of the water column.

The  $L_u(0^-)$  results (Fig. 15a) show the lowest uncertainties with the Satlantic processor are for the shallow coastal data, and in all cases, the largest uncertainties are for the red wavelengths—none of the Satlantic uncertainties are below 1.0%, although, the blue-green WiSPER wavelengths are within 2.5%. Better agreement in the shallow coastal (predominantly Case-2) data rather than the deep ocean (Case-1) data is unexpected, but it has a simple explanation: the shallow water depth constrains the options for selecting the extrapolation interval.

The JG uncertainties are always below 2.5%, and mostly below 1.0% except for the blue and red SeaOPS data. The  $K_d$  uncertainties (Fig. 15b) show much higher overall uncertainties with respect to the Satlantic processor, particularly for the LoCNESS data set where every wavelength has an uncertainty above 25%. None of the Satlantic uncertainties are below 2.5%, whereas all of the JG uncertainties are, and most of the JG uncertainties are to within 1.0% (the primary exception are the WiSPER data). These results suggest a database constructed with processed data from a wide source of contributors will have substantially higher uncertainties than a database constructed with raw data which is processed with a single processor, although band ratios regularly provide reduced uncertainties with respect to individual spectral uncertainties.

To minimize observational uncertainties, the SeaWiFS Project has sponsored a variety of multidisciplinary workshops to outline the observations and sampling protocols

required for bio-optical algorithm development (Mueller and Austin 1992 and 1995). One of the consequences of the workshops was the establishment of the series of the aforementioned SIRREX activities to demonstrate and advance the state of the art for calibrating the instruments used in field activities. Although prior SIRREX activities significantly reduced the uncertainties in optical calibrations, some important sources of uncertainty were not quantified. One of the most important of these, from the vantage of the calibration equation, was the immersion factor.†

For commercial radiometers, the raw data are converted to physical units based on a formulation given by the manufacturer. For Satlantic sensors, the  $i$ th sample for a radiometer at center wavelength  $\lambda$ , are converted to physical units according to the following equation:

$$\mathfrak{C}(\lambda, t_i) = C_c(\lambda) I_f(\lambda) [V(\lambda, t_i) - \bar{D}(\lambda)], \quad (3)$$

where  $\mathfrak{C}(\lambda, t_i)$  is the calibrated value ( $\mathfrak{C}$  is replaced by  $E_d(z)$ ,  $E_u(z)$ ,  $L_u(z)$ , or  $E_d(0^+)$  depending on the sensor type),  $C_c(\lambda)$  is the calibration coefficient,  $I_f(\lambda)$  is the immersion factor,  $V(\lambda, t_i)$  is the raw voltage (in digital counts) measured by the instrument at time  $t_i$  (which also sets the depth,  $z$ ), and  $\bar{D}(\lambda)$  is the average dark value (in digital counts) measured during a special *dark cast* with the caps on the radiometer.

The immersion factor is a first-order term in the sense that the uncertainty in this term is represented at the same level as the calibration coefficient, so the the final uncertainty of the calibrated data is heavily dependent on the uncertainty in the immersion factor. For irradiance sensors, the immersion factor is determined experimentally. A suggested and acceptable procedure is as follows (Mueller and Austin 1995):

1. The instrument is placed in a tank of water with all surfaces painted black.
2. The sensor is leveled with the irradiance collector plate facing upward.
3. A tungsten-halogen lamp with a small filament, powered by a stable power supply, is placed at some distance above the water surface.
4. An initial reading is taken with the water level below the collector, i.e., with the collector in the air and dry.
5. The depth of the water is increased in steps and readings are recorded for all wavelengths from each carefully measured depth.

Note that in most cases, water is removed from the tank with a pump, and data are usually recorded inbetween pumping intervals.

---

† The coefficient accounting for the change in sensor responsivity when the in-air calibration is applied to in-water measurements ( $I_f = 1$  for above-water sensors).

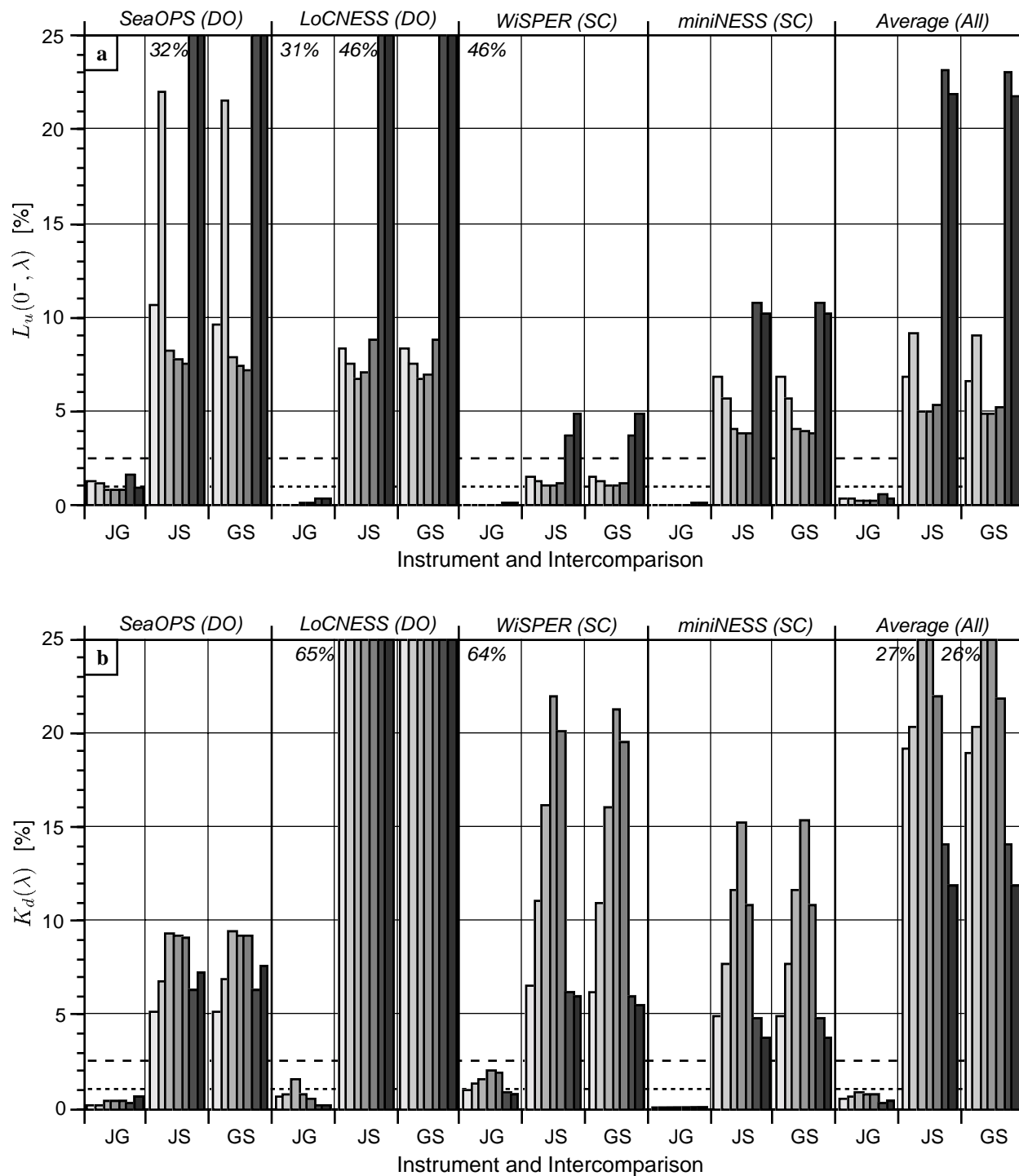


**Fig. 5.** The average processing uncertainties for the JG, JS, and GS intercomparisons of **a)**  $L_u(0^-)$  and **b)**  $K_d$ . The dashed line sets the 2.5% intercomparison objective and the dotted line the 1.0% objective. Uncertainties above 25% are shown clipped at the 25% level, and the maximum uncertainty achieved is given at the top of the panel to the side of the clipped bars. The individual wavelengths are shown as the sequential bars with varying intensities of gray (going from left to right, blue is light gray and red is dark gray). The instrument (and deployment location) codes are given along the top of the subpanels. The overall average of all the data (40 casts) is given in the right-most three intercomparisons.

The amount of energy arriving at the collector varies with the water depth and is a function of several factors: a) the attenuation at the air-water interface, which varies with wavelength, b) the attenuation over the water path-length, which is a function of depth and wavelength; and c) the change in solid angle of the light leaving the source and arriving at the collector, caused by the light rays changing direction at the air-water interface, which varies with wavelength and water depth. When all of these effects are properly accounted for, the immersion factor can be computed.

The SIRREX-8 activity is taking place during the last three months of 2001 and is concerned with the round-robin determination of immersion factors for 9 Satlantic radiometers at three different calibration facilities. A picture of the tank used at the first facility, the Center for Hydro-Optics and Remote Sensing (CHORS), from 28 September to 9 October 2001 is shown in Fig. 6. The other two facilities will be the JRC and Satlantic. All of the data will be processed by the JRC to ensure there are no extra uncertainties as a result of differences in data processing methods.



**Fig. 6.** The water tank used at the CHORS calibration facility for measuring immersion factors. The radiometer is set inside a large tube atop an aluminum grate that is covered in a fine mesh. The mesh helps dissipate the turbulence caused by the addition or removal of water.

A preliminary comparison of the immersion coefficients for a sensor used during the first phase of SIRREX-8 at CHORS is shown in Fig. 7. For the CHORS work, one radiometer, an  $E_u$  sensor (S/N 130), was selected as a baseline instrument and was subjected to a variety of experiments and trials. The data shown in Fig. 7 are for three of the trials when the amount of particles in the tank

was kept very low (clean water conditions ensure the surface reflectance is in keeping with the Fresnel reflectance assumption).

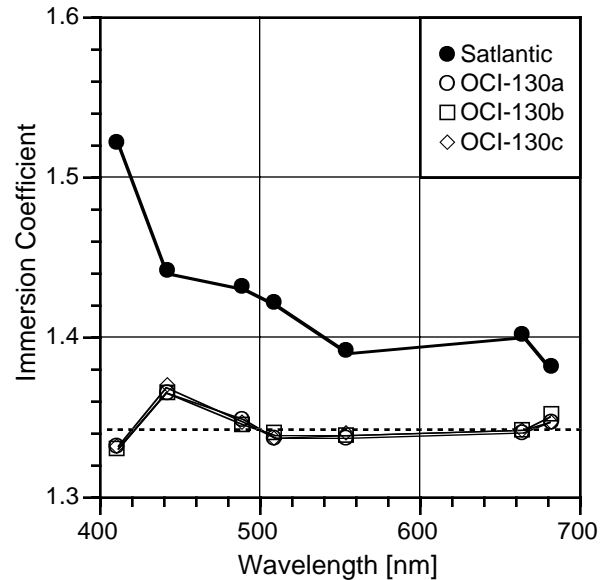


**Fig. 7.** The immersion coefficients supplied by Satlantic (filled circles) and as determined with the JRC data processor from the CHORS data during SIRREX-8 for  $E_u$  sensor S/N 130 for three days of measurements (open circles). The dashed line is the average immersion coefficient from the three CHORS measurements.

The CHORS data show excellent agreement between trials and good agreement with respect to the average value from the three days of data. The latter is an important point, because the *a priori* expectation is that the immersion coefficients should be spectrally uniform. The CHORS data shows this is basically the case, except in the blue where the values at 412 nm are depressed and the values at 443 nm are elevated. The Satlantic values show a much greater spectral dependence with maximal values in the blue, decreasing through the green, and then minimal in the red. The differences between the Satlantic and CHORS data are significantly large, i.e., they are much larger than the 2% uncertainty demonstrated for Satlantic irradiance sensors during SIRREX-7 (Hooker et al. 2001b). The immersion coefficients can be considered as percentages, so the maximum differences in the blue, green, and red are approximately 19, 8, and 6%, respectively.

Most manufacturers, Satlantic included, do not characterize the immersion coefficients for each instrument they produce, because of the time (and thus cost) involved in the extra laboratory work. The standard technique described above requires approximately 2 hr to complete one realization. Assuming three trials are an acceptable minimum for characterization work, this means almost one day of laboratory time would have to be added to the cost of

each instrument. Consequently, instrument manufacturers rely on characterizing a class of diffuser designs and then assigning the immersion factors to all instruments manufactured within the class.

The SIRREX-8 preliminary results suggest the class characterization approach is questionable and a considerable amount of effort is needed to recharacterize the instruments being used in calibration and validation activities. In any effort to lower the cost involved, one of the objectives of SIRREX-8 was to test a new procedure that can be executed in one-sixth the time of the standard method.

## Planned Activities and Schedule

This is the last year of the funded activity. Calibrated data of sufficient quality is just now becoming available, but unfortunately, it does not overlap with any of the field campaigns discussed in this report. When additional processed data becomes available that does coincide with field campaigns described here and in previous reports, match ups with these data will be made on an ad hoc basis.

## Data Archive and Access

SeaWiFS Field Team optical and pigment data are stored in the SeaWiFS Bio-Optical Archive and Storage System (SeaBASS) which is a well documented archival system (Hooker et al. 1994). The data are available to authorized users (which includes all those who contribute to the database), but cannot be made public or published without prior approval or participation of the owner (Hooker et al. 1993).

## Publications (Last 12 Months)

- Aiken, J., N. Rees, S. Hooker, P. Holligan, A. Bale, D. Robins, G. Moore, R. Harris, and D. Pilgrim, 2000: The Atlantic Meridional Transect; Overview and Synthesis of Data. *Prog. Oceanogr.*, **45**, 257–312.
- Behrenfeld, M.J., E. Marañón, D.A. Siegel, and S.B. Hooker, 2000: Resolving the “Missing Biology” in Bio-Optical Models of Primary Production. *Limnol. Oceanogr.*, (in press).
- Claustre, H., A. Morel, S.B. Hooker, M. Babin, D. Antoine, K. Oubelkheir, A. Bricaud, K. Leblanc, B. Quéguiner, and S. Maritorena. 2001. Is desert dust making oligotrophic waters greener? *Geophys. Res. Lett.*, (submitted).
- Firestone, E.R., and S.B. Hooker, 2001: SeaWiFS Postlaunch Technical Report Series Cumulative Index: Volumes 1–11. *NASA Tech. Memo. 2001–206892, Vol. 12*, S.B. Hooker and E.R. Firestone, Eds., NASA Goddard Space Flight Center, Greenbelt, Maryland, 24 pp.
- Hooker, S.B., and G. Lazin, 2000: The SeaBOARR-99 Field Campaign. *NASA Tech. Memo. 2000–206892, Vol. 8*, S.B. Hooker and E.R. Firestone, Eds., NASA Goddard Space Flight Center, 46 pp.
- , and S. Maritorena, 2000: An Evaluation of Oceanographic Optical Instruments and Deployment Methodologies. *J. Atmos. Oceanic Technol.*, **17**, 811–830.

- , and C.R. McClain, 2000: A Comprehensive Plan for the Calibration and Validation of SeaWiFS Data. *Prog. Oceanogr.*, **45**, 427–465.
- , and A. Morel, 2001: Platform and Environmental Effects on Above- and In-Water Determinations of Water-Leaving Radiances. *J. Atmos. Ocean. Tech.*, (submitted).
- , G. Lazin, G. Zibordi, and S. McLean, 2001: An Evaluation of Above- and In-Water Methods for Determining Water-Leaving Radiances. *J. Atmos. Oceanic Technol.*, (accepted).
- , N.W. Rees, and J. Aiken, 2000: An Objective Methodology for Identifying Oceanic Provinces. *Prog. Oceanogr.*, **45**, 313–338.
- , G. Zibordi, J-F. Berthon, S. Bailey and C. Pietras, 2000: The SeaWiFS Photometer Revision for Incident Surface Measurement. *NASA Tech. Memo. 2000–206892, Vol. 11*, S.B. Hooker and E.R. Firestone, Eds., NASA Goddard Space Flight Center, Greenbelt, Maryland, 24 pp.
- , S. Maritorena, G. Zibordi, and S. McLean, 2001: Results of the Second SeaWiFS Data Analysis Round-Robin, March 2000 (DARR-00). *NASA Tech. Memo. 2000–206892, Vol. 14*, S.B. Hooker and E.R. Firestone, Eds., NASA Goddard Space Flight Center, Greenbelt, Maryland, (in press).
- , H. Claustre, J. Ras, L. Van Heukelem, J-F. Berthon, C. Targa, R. Barlow, and H. Sessions, 2000: The First SeaWiFS HPLC Analysis Round-Robin Experiment (SeaHARRE-1). *NASA Tech. Memo. 2000–206892, Vol. 14*, S.B. Hooker and E.R. Firestone, Eds., NASA Goddard Space Flight Center, Greenbelt, Maryland, 42 pp.
- , S. Maritorena, G. Zibordi, and S. McLean, 2001: Results of the Second SeaWiFS Data Analysis Round-Robin, March 2000 (DARR-00). *NASA Tech. Memo. 2001–206892, Vol. 15*, S.B. Hooker and E.R. Firestone, Eds., NASA Goddard Space Flight Center, Greenbelt, Maryland, (in press).
- , S. McLean, J. Sherman, M. Small, G. Zibordi, and J. Brown, 2001: The Seventh SeaWiFS Intercalibration Round-Robin Experiment (SIRREX-7), March 1999. *NASA Tech. Memo. 2000–206892, Vol. 16*, S.B. Hooker and E.R. Firestone, Eds., NASA Goddard Space Flight Center, Greenbelt, Maryland, (in press).
- Zibordi, G., S.B. Hooker, J-F. Berthon, and D. D’Alimonte. 2001. Autonomous above-water radiance measurements from an offshore platform: A field assessment experiment. *J. Atmos. Ocean. Tech.*, (accepted).

## References

- Aiken, J., N.W. Rees, S. Hooker, P. Holligan, A. Bale, D. Robins, G. Moore, R. Harris, and D. Pilgrim, 2000: The Atlantic Meridional Transect: overview and synthesis of data. *Prog. Oceanogr.*, **45**, 257–312.
- Austin, R.W., 1974: “The Remote Sensing of Spectral Radiance from Below the Ocean Surface.” In: *Optical Aspects of Oceanography*, N.G. Jerlov and E.S. Nielsen, Eds., Academic Press, London, 317–344.
- Hooker, S.B., and W.E. Esaias, 1993: An overview of the SeaWiFS project. *Eos, Trans., Amer. Geophys. Union*, **74**, 241–246.

- , W.E. Esaias, and L.A. Rexrode, 1993: Proceedings of the First SeaWiFS Science Team Meeting. *NASA Tech. Memo. 104566, Vol. 8*, S.B. Hooker and E.R. Firestone, Eds., NASA Goddard Space Flight Center, Greenbelt, Maryland, 61 pp.
- , C.R. McClain, J.K. Firestone, T.L. Westphal, E-n. Yeh, and Y. Ge, 1994: The SeaWiFS Bio-Optical Archive and Storage System (SeaBASS), Part 1. *NASA Tech. Memo. 104566, Vol. 20*, S.B. Hooker and E.R. Firestone, Eds., NASA Goddard Space Flight Center, Greenbelt, Maryland, 40 pp.
- , and J. Aiken, 1998: Calibration evaluation and radiometric testing of field radiometers with the SeaWiFS Quality Monitor (SQM). *J. Atmos. Ocean. Tech.*, **15**, 995–1,007.
- , and S. Maritorena, 2000: An evaluation of oceanographic radiometers and deployment methodologies. *J. Atmos. Ocean. Technol.*, **17**, 811–830.
- , and C.R. McClain, 2000: The Calibration and Validation of SeaWiFS Data. *Prog. Oceanogr.*, **45**, 427–465.
- , G. Zibordi, J-F. Berthon, S.W. Bailey, and C.M. Pietras, 2000: The SeaWiFS Photometer Revision for Incident Surface Measurement (SeaPRISM) Field Commissioning. *NASA Tech. Memo. 2000–206892, Vol. 13*, S.B. Hooker and E.R. Firestone, Eds., NASA Goddard Space Flight Center, Greenbelt, Maryland, 24 pp.
- , S. Maritorena, G. Zibordi, and S. McLean, 2001a: Results of the Second SeaWiFS Data Analysis Round-Robin, March 2000 (DARR-00). *NASA Tech. Memo. 2001–206892, Vol. 15*, S.B. Hooker and E.R. Firestone, Eds., NASA Goddard Space Flight Center, Greenbelt, Maryland, (in press).
- , S. McLean, J. Sherman, M. Small, G. Zibordi, and J. Brown, 2001b: The Seventh SeaWiFS Intercalibration Round-Robin Experiment (SIRREX-7), March 1999. *NASA Tech. Memo. 2001–206892, Vol. 16*, S.B. Hooker and E.R. Firestone, Eds., NASA Goddard Space Flight Center, Greenbelt, Maryland, (in prep.).
- Joint Global Ocean Flux Study, 1991: JGOFS Core Measurements Protocols. *JGOFS Report No. 6*, Scientific Committee on Oceanic Research, 40 pp.
- Loisel, H., and A. Morel, 1998: Light scattering and chlorophyll concentration in case 1 waters: A reexamination. *Limnol. Oceanogr.*, **43**, 847–858.
- Mobley, C.D., 1999: Estimation of the remote-sensing reflectance from above-surface measurements. *Appl. Opt.*, **38**, 7,442–7,455.
- Morel, A., 1980: In-water and remote measurements of ocean color. *Bound.-Layer Meteorol.*, **18**, 177–201.
- , and B. Gentili, 1996: Diffuse reflectance of oceanic waters, III. Implication of bidirectionality for the remote sensing problem. *Appl. Opt.*, **35**, 4,850–4,862.
- Mueller, J.L., 2000: “Overview of Measurement and Data Analysis Protocols” and “In-water radiometric profile measurements and data analysis protocols.” In: Fargion, G.S., and J.L. Mueller, Ocean Optics Protocols for Satellite Ocean Color Sensor Validation, Revision 2. *NASA Tech. Memo. 2000–209966*, NASA Goddard Space Flight Center, Greenbelt, Maryland, 87–97.
- , and R.W. Austin, 1992: Ocean Optics Protocols for SeaWiFS Validation. *NASA Tech. Memo. 104566, Vol. 5*, S.B. Hooker and E.R. Firestone, Eds., NASA Goddard Space Flight Center, Greenbelt, Maryland, 43 pp.
- , and —, 1995: Ocean Optics Protocols for SeaWiFS Validation, Revision 1. *NASA Tech. Memo. 104566, Vol. 25*, S.B. Hooker, E.R. Firestone, and J.G. Acker, Eds., NASA Goddard Space Flight Center, Greenbelt, Maryland, 66 pp.
- , B.C. Johnson, C.L. Cromer, S.B. Hooker, J.T. McLean, and S.F. Biggar, 1996: The Third SeaWiFS Intercalibration Round-Robin Experiment, SIRREX-3, September 1994. *NASA Tech. Memo. 104566, Vol. 34*, S.B. Hooker, E.R. Firestone, and J.G. Acker, Eds., NASA Goddard Space Flight Center, Greenbelt, Maryland, 78 pp.
- Siegel, D.A., M.C. O’Brien, J.C. Sorensen, D.A. Konnoff, E.A. Brody, J.L. Mueller, C.O. Davis, W.J. Rhea, and S.B. Hooker, 1995: Results of the SeaWiFS Data Analysis Round-Robin (DARR-94), July 1994. *NASA Tech. Memo. 104566, Vol. 26*, S.B. Hooker and E.R. Firestone, Eds., NASA Goddard Space Flight Center, Greenbelt, Maryland, 58 pp.
- Zibordi, G., J.P. Doyle, and S.B. Hooker, 1999: Offshore tower shading effects on in-water optical measurements. *J. Atmos. Ocean. Tech.*, **16**, 1,767–1,779.
- , S.B. Hooker, J-F. Berthon, and D. D’Alimonte. 2001. Autonomous above-water radiance measurements from an offshore platform: A field assessment experiment. *J. Atmos. Ocean. Tech.*, (accepted).